Non-collision Injuries In Urban Buses

– Strategies For Prevention

Alejandro Palacio[a], Giuseppe Tamburro[a], Desmond O'Neill[b] and Ciaran K Simms[a*]

[a] *Centre for Bioengineering, Parsons Building, Trinity College, College Green, Dublin 2, Ireland.*
[b] *Dept. of Medical Gerontology, Trinity Centre for Health Sciences, Adelaide and Meath Hospital, Tallaght, Dublin 24, Ireland.*

Abstract

Public transport is a potentially important part of independent living for older people, but they are over-represented in non-collision bus injuries. This paper reports on a computational modelling approach to addressing this problem: the Madymo human model validated for simulating passive, seated vehicle occupants was adapted to simulate a standing passenger in an accelerating bus. The force/deformation characteristics of the bus were measured and the human model was expanded to include a validated active hand grip. Real world urban bus acceleration profiles were measured and used as inputs for the simulations. Balance loss could not be predicted, but injuries from contact with the vehicle floor following a fall were evaluated.

---

[*] Corresponding Author: Tel.: +353-1-8963768; fax: +353-1-6795554.
Email address: csimms@tcd.ie (C.K. Simms).

Results show that peak bus accelerations measured ($\pm$0.32g) exceed reported acceleration thresholds for balance loss for a standing passenger using a handgrip (0.15g).

The maximum predicted probability of knee and head injuries arising from impact with bus seats, handrails and walls were 53% and 35% respectively. The stairwell and horizontal seatback handles were particularly hazardous and the latter should be replaced with vertical handrails. Driver training should be expanded to include video training based on multibody simulations to highlight the risks for standing passengers induced by harsh braking and acceleration.

1. Introduction

In many societies, the proportion of older people is rising and transportation is important to health, social inclusion and maintaining older adult independence (O'Neill and Carr, 2006). However, problems with transportation for older people have been recognized (Canavan et al., 2005). Public transport is a transport modality with important societal benefits, but a number of design and suitability issues have so far resulted in a relatively low uptake of this option by older people in many developed countries (Ling Suen and Sen, 2004). Even so, there is a suggestion that among older age groups (over 75s) service usage has begun to increase (Golob and Hensher, 2007). In the developing world, where the majority of older people live, relatively higher numbers of older people travel by bus (Odufuwa, 2006).

Design of public transport tends to be service rather than user-led, and although recent improvements in bus design allow less mobile people to make use of bus travel, our review of the literature will show that older people are particularly vulnerable to non-collision bus injuries (injuries that occur while travelling on a bus without the bus itself being involved in a collision). There is therefore a dual imperative to characterize the factors underlying the risks associated with public transportation for older people: resolution of the increased injury risk is important for existing users, but risk reduction should also increase the proportion of older people using public transport, thereby improving social inclusion and independence levels.

1.1. Overview of bus non-collision injuries

Most bus passenger injuries are due to falls (Fruin et al., 1994) and a preliminary study from our group found that older people are disproportionately represented in non-collision bus injuries in south-west Dublin, Ireland (Canavan et al., 2005). In the UK, Kirk et al. (2001) used British national road accident data ('STATS 19') and in-depth cases to study the demographics of the bus and coach casualty population. They concluded that occupants fall due to slipping or tripping on poorly designed floor surfaces, in wet weather conditions or due to inertial forces as the bus brakes or accelerates, see Fig. 1. When these falls occur, the design of the interior substantially affects injury risk. Standing passengers are the most injured (887 cases) after sitting passengers (1326 cases). The age and gender of passengers injured (Fig. 1) is strongly related to their travel frequency, with children/teenagers and passengers over 60 years old being overrepresented.

3

In Israel, Halpern et al. (2005) assessed non-collision injuries on urban and rural buses. Of 120 patients (86 females, 34 males; aged 3-89 years) with non-collision injuries sustained on a public bus, the majority (55.8%) were over 55 years of age and most injuries were sustained on inner-city trips by passengers who were standing or moving. The most common mechanism of injury (52.5%) was sudden acceleration, and the main injuries were to the limbs (33.3%), head (29%) and spine (22%).

In Sweden, Albertsson (2005 a,b) reported a ten-year study analyzing 284 injured bus and coach occupants. The majority of incidents were non-collision injuries (154 incidents, 54%), with an increase of 24% in the last ten years. Two types were identified: alighting/boarding while the bus was stationary (37%) and balance loss while the bus was moving (17%). Of these, considering MAIS2 cases, 28% occurred during harsh braking and 27% in acceleration from standstill, but the body regions injured are not reported. Most cases involved females (77%) and the mean age was 42 for those injured in a moving bus, lower than reported by Kirk et al. (2001). More than half (54%) were injured because the bus was braking or accelerating and most of the remaining 46% were injured due to balance loss while moving in the bus. The injuries sustained were evenly distributed to the upper extremities (27%), head (23%) and the lower extremities (21%).

In an early review paper, Fruin et al. (1994) reported that cuts, grazes and bruises to the head or neck were frequent when entering and leaving seats. They recommended no standees in the aisles, eliminating high steps, obstacles, inadequate grab handles, and poor floor design, and increasing illumination to reduce the chance of falls. They also suggested minimizing the effects of secondary impacts by ensuring interior surfaces are padded adequately and suggested driver training.

In summary, non-collision injuries on buses represent a significant source of injuries, with older female passengers at particular risk. Head and lower extremity injuries are the most frequent in non collision accidents and harsh speed changes are a frequent cause of this. However, so far there has been no biomechanical analysis of non-collision injuries on buses and the mechanisms of injury are therefore poorly understood.

2. Objectives

This paper presents a crash simulation approach aimed at improving our understanding of non collision injuries on urban buses. The goal is to predict injuries sustained by a standing passenger in the event of a fall during everyday traffic. This required altering the existing Madymo passive human occupant model to facilitate balance and active gripping as well as the measurement of urban bus acceleration profiles to provide input data for the simulations. The simulation results could then used together with injury criteria to predict the relationship between vehicle acceleration, design and occupant injury likelihood in the event of a fall.

3. Methods

3.1. Basic balance model for human standing

The inherent instability of human balance is seen by considering a forward facing standing passenger as a rigid lamina of width *2b* and height *H* acted on by gravity and point

reaction forces F_1 and F_2 from the floor acting at the front and back of the shoes respectively. The height of the centre of gravity from the the floor is h. If μ is the shoe/floor contact friction coefficient and $\ddot{x}_{B_{MAX}}$ is the maximum bus acceleration a standing occupant can withstand without falling over, the limiting condition for balance is $\mu = b/h$, ie passive balance depends only on the geometry of the lamina. When $\mu > b/h$, the lamina tends to fall over. For a 50th percentile male, the centre of gravity lies slightly below the belly button and the average ratio of center of mass height to overall height (h/H) is ≈ 0.56 (Gambino et al., 2006). The 50th percentile male Madymo height is 1.74m (TNO, 2006) and h is therefore 0.97m. For a midbody width ($2b$) of approximately 0.4m, $b/h \approx 0.2$. In contrast, the friction coefficient (μ) between the shoes and bus floor is almost always greater than this (μ=0.85 for dry and clean floors and μ=0.49 for dry and dirty floors, according to Sigler (1943)). Therefore the maximum bus acceleration a "passive" standing passenger can withstand without holding on or taking corrective action is approximately 0.2g. Normally, bus passengers do not fall because they take corrective action, but the literature review has shown that falls in moving buses are frequent events. The science of human balance is very complex and will not be directly addressed in this paper: a simplification to address this issue will be described instead.

3.2. Detailed Human Body Model for injury prediction

The Madymo Human Body Model (HBM) database features a 5th percentile female (height = 1.52m, mass = 49.8kg), a 50th percentile male (1.74m , 75.7kg) and a 95th

percentile male (1.91m , 101.1kg) (TNO, 2006). Therefore, the 50th percentile male facet HBM was chosen to simulate a standing bus passenger because it is closest to the US 50th percentile female anthropometrics (1.625m, 65kg) (Pheasant and Haslegrave, 2006). This multibody model has lumped joint parameters and a finite element skin surface with null material properties for contact detection and visualization. Normally, validation of numerical models using experimental tests is desirable. However, it was not feasible to perform tests with a physical dummy on a bus, and instead the Madymo HBM was chosen in preference to a crash dummy model because of its increased biofidelity and because it has been validated at both component and whole-body level using volunteer and cadaver experiments in a variety of impact scenarios (TNO, 2006). However, two modifications to facilitate application as a standing bus occupant were required: (1) development of an active hand model to simulate the grip onto a handrail and (2) a means of replicating balance during quiet standing.

3.3. Hand model development

The bones of the hand are represented by rigid bodies. The interphalangeal and metacarpal joints were assumed to be flexion/extension hinge joints: restraints limit the joint ranges of motion and stiff belt segments model the tendons, with locations taken from the literature (An, 1979). The main finger flexor muscles (flexor digitorum profundus and flexor digitorum superficialis) were combined into one single representative Hill type muscle with cross-sectional area and length derived from Lieber et al. (1992). The maximum active muscle stress ($86N/cm^2$) reported by Buchanan et al. (2004) was used.

The hand model was validated for grip force by simulating experiments in which a hand dynamometer was used to measure static grip force for males and females over a range of ages (Mathiowetz, 1985): the average grip strength for males aged 45-49 was 488N. A model of the hand dynamometer was developed in Madymo and the peak simulated grip force was 490N. Since the model represents a 50%^{ile} adult male hand, there was very close correspondence between the model and the experimental data, and no "tuning" was performed. However, grip strength deteriorates with age (Mathiowetz, 1985): the average reported grip for males above 65 years was only 343N. Therefore, the hand grip of an older person was represented by scaling the maximal muscle stress parameter by a factor of 343/488.

3.4. Madymo model stability system

Balance requires closed loop control using neural signals to activate muscles to generate a complex sway movement. Replicating this mechanism was not feasible as muscle activation data is not readily available due to signal-to-noise ratio problems at low muscle activation levels. Therefore a simpler solution was devised: the hip, knee and ankle joint torques required for quiet standing were determined from the model (from the static case) and additional torque-angle restraints were implemented in the hip, knee and ankle to generate these torques in quiet standing. In the simulations, a switch was used to remove these restraints when falling over has initiated. This solution cannot model active balance, but it stabilises the standing HBM in the absence of a perturbation and hence facilitates

simulation of injury mechanisms resulting from a fall given that balance loss has been initiated.

3.5. Bus model

The interior of a common urban bus was created using planes, cylinders and ellipses (Fig. 2). For contact with the walls, handrails and seat bases, only the contact characteristics of the Madymo HBM were used because of the large stiffness disparity between the body and these bus surfaces. The calculations for the shoe floor contact characteristic are shown in Appendix A. The contact friction coefficient is important and each scenario was modelled using two floor conditions: $\mu_1=0.85$ for a dry and clean floor and $\mu_2=0.49$ for a dry and dirty floor. Rubber-soled footwear was assumed. Preliminary simulations showed leg injures were mostly caused by contact with the seats, and the load-deformation characteristics of a typical bus seat were determined, with separate tests for the seat metal frame joint angular stiffness, the bending behaviour of the seat metal frame and the deformation of the seat cushion foams, see Appendix B.

3.6. Measuring system for bus acceleration profiles

A portable system consisting of a capacitive accelerometer (*PCB Piezotronics Y3801G3FB3G/030DZ SN 1327)* connected to a laptop was developed to measure the horizontal acceleration of buses. Data were recorded during ten trips on different bus urban routes with the accelerometer fixed to the bus floor via a high friction contact and pressure

from the foot. Drivers were not aware of this procedure. The laptop was positioned on the knees, and a Labview program allowed measurement of the acceleration time history and insertion of real-time commentary on the driving manoeuvres. The data were subsequently low-pass filtered (at 12.5Hz) in Matlab to yield acceleration input curves for the Madymo simulations.

3.7. Injury Criteria

Injury criteria developed from experimental tests on cadavers/volunteers are required to relate mechanical loading to the probability of sustaining injury. Following the literature review, this study focused on the head and lower extremities. The injury criteria and threshold values (Eppinger et al., 1999; Funk et al., 2002; Ivarsson et al., 2004; Kerrigan et al., 2004) are summarized in Table 1 and Table 2, where injuries have been categorised using the Abbreviated Injury Scale (AIS). Due to the inherent variability in biomechanical impact testing, Weibull cumulative distribution functions have been applied:

$$W(z, \alpha, \beta, \gamma) = 1 - e^{-(z - \gamma / \alpha)^{\beta}}$$, where α (> 1) is the scale parameter, β (>1) is the shape parameter and γ is the location parameter. Using this method, injury risk curves were developed for each type of injury, see Tables 1 and 2. For the Head Injury Criterion (HIC) a standard normal cumulative function was used. In cases where two threshold values were established, these are the minimum and maximum values found in the literature.

Deterioration of bone strength after the age of fifty has been well documented in tests on femoral cortical bone (Takahashi et al., 2000; Yamada, 1970). Similarly, theoretical age

dependent HIC scaling factors have been proposed based on brain material properties (Eppinger et al., 1999). However, there is no published data relating to failure stress of brain tissue with old age (Eppinger et al., 1999) and therefore it is not yet possible to quantify the increased risk to an older female compared to a 50th percentile male occupant. The injury risk to the 50th percentile male model presented in this paper is therefore probably a best case scenario, and the risk to an older female may be higher.

4. Results

There are two groups of results: acceleration profiles obtained during regular trips on urban buses in a European city and passenger injury probabilities predicted by the bus occupant simulation model.

4.1. Real world acceleration/deceleration pulses

On each trip, bus acceleration patterns were recorded continuously for periods of approximately five minutes. Events such as starting and stopping at bus stops/traffic lights and unexpected braking were annotated in real-time. In subsequent analysis, time periods showing high peaks in acceleration/deceleration were identified and critical pulses of 4-5 second duration were extracted. Three of the most representative of these were used as inputs for the subsequent Madymo simulations (Fig. 3):

- MEASURE 1.1 a bus travelling at constant speed followed by harsh braking (a maximum value of -0.32g) while approaching a traffic light.

- MEASURE 2.1 a bus accelerating from a bus-stop to a constant speed. There is a short period of deceleration in the mid span due to soft braking. A peak acceleration value of 0.16g was reached after 5.3 seconds.

- MEASURE 2.4 is a high acceleration followed by a long deceleration measured on a bus accelerating quickly from a traffic light and then suddenly braking to a halt because of traffic congestion. This was a very common situation. A peak positive value of 0.14g was reached at the beginning when the bus is accelerating, which then decreased constantly until the bus brakes. Although the peak values are not the highest measured overall, these fast changes may be significant for occupant balance.

4.2. Passenger kinematics and injury probabilities

After observing passenger standing behaviour, two positions were identified as being commonly occupied by standing passengers in urban buses (Fig. 2). In "Position 1" a standing passenger is grasping a horizontal handrail to maintain equilibrium. In "Position 2" a passenger is standing and holding a centrally located vertical handrail. Seven non-collision accident configurations were simulated. These were differentiated by the position of the occupant ("Position 1" or "Position 2"), the acceleration pulse ("MEASURE 1.1", "MEASURE 2.1" or "MEASURE 2.4") and the shoe/floor friction coefficient ($\mu = 0.49$ (A) or $\mu = 0.85$ (B)). The simulation matrix is summarized in Table 3. Euler integration with a

constant time-step of 1exp-6s was used in all simulations. From all the results obtained

corresponding to head, femur, knee and tibia injuries, Table 4 summarises the most

representative values. These results will be referred to in detail in section 5.3.

5. Discussion

It has been shown in the literature review that non collision accidents are responsible for

a large proportion of injuries in older bus passengers. In this paper real-world

acceleration/deceleration patterns of urban buses in daily traffic were measured and used as

inputs to a multi-body bus-occupant simulation model and the likely biomechanical causes

of injuries were evaluated.

5.1. Model assumptions, limitations and validity

The validity of the injury response model is based on the extensive validation of the

Madymo 50th percentile male occupant model in frontal and rear impact eg (Don et al.,

2003; Happee et al., 1998; Kroonenberg et al., 1998) and of the detailed Madymo leg

model (Funk, 2001; Funk, 2002; Manning, 1998). The hand model developed in this paper

accurately reproduces the grip strength measured on volunteers (Mathiowetz, 1985).

Human balance is known to involve a complex active feedback mechanism, and strategies

such as the *hip*, *ankle* and *stepping strategies* to prevent a fall in the event of a perturbation

have been identified (Lord et al., 2001). In some cases, these prevent balance loss but the

literature shows that falls are frequent occurrences. In the present work, balance strategies

13

have not been implemented, and the simulations are not intended to predict the occurrence of balance loss. Rather, they predict the kinematics and subsequent injuries given that balance loss has been initiated following bus braking/accelerating.

The variations of injury risk with age and sex are well known (Eppinger, 1999; King, 2001; Meserer, 1880; Yamada, 1970) but as stated in the methods section, it is not yet possible to quantify the increased risk to an older female compared to a 50th percentile male occupant. The injury risk to the 50th percentile male model presented in this paper is therefore a best case scenario and the risk to an older female is expected to be higher.

Therefore the causes and distribution of injuries given that a fall has occurred can be assessed using the approach adopted in this paper. This approach facilitates the development of biomechanically based design improvement strategies for bus interiors, as well as driver training aids. The model has been used to simulate three separate acceleration pulses, two different standing occupant positions and in the analysis of the influence of the shoe/floor friction.

5.2. Bus acceleration measurements

The three real-world pulses used as inputs for the simulations were chosen to represent common situations in daily traffic (Fig. 3). These pulses lasted less than 5 seconds, since the time that the human model needed to fall to the ground was around 2.5 seconds. The peak positive acceleration measured was ≈0.2g, and the peak negative acceleration was 0.32g measured during a harsh braking manoeuvre. De Graaf and Van Weperen (1997) measured acceleration levels during travel in urban buses in Amsterdam and found initial

accelerations of 0.1-0.2g and a peak acceleration of 0.215g which is in good agreement with the results presented here. This indicates similar vehicle driving patterns in the two studies and that the findings presented here from one specific urban region can be generalised to other urban regions.

5.3. Computer simulations

During simulations performed in 'Position 1', the three different input pulses were used (Table 3), so the results are analyzed separately. Simulation 1A (Fig. 4) represents an urban bus travelling at constant velocity followed by harsh braking as a traffic light is approached. Due to inertia, the standing passenger moves forward relative to the braking bus and the model leg impacts the lateral seat border. Following this, the head and right arm contact with the stairs wall. The severity of the head impact is greatly reduced due to the primary impact between the leg and the seat. However, the wall in double-decker buses separating the stairs from the rest of the standing area is identified as a high risk element for head injuries that could lead to skull fractures (indicated by Simulation 1A). In addition, contact between the leg and the stiff seat produced a high bending torque in the right knee close to the lower threshold limit, with a 20% probability of knee failure. (Ivarsson et al. (2004) performed failure tests on intact knee specimens subjected to symmetric valgus 4-point bending and defined knee failure as failure of the medial collateral ligament (Vilenius et al., 1994))

Simulations 2A and 2B have the same acceleration pulse representing a bus accelerating to a constant velocity from a bus stop, but have different friction coefficients between the

15

shoes and the bus floor. The first case (2A) resulted in a large HIC value (HIC_{15} measured was 758, threshold is 700) due to impact of the passenger's head with the upper metal handle in the seatback. This represents a 35% risk of skull fracture, according to threshold values established for the 50%th percentile male. There is also a high lateral-medial bending torque in the left tibia as a consequence of contact between the leg and the front seat border. The Tibia Index (TI) calculated for this case was the highest obtained in any of the simulations (TI = 1.2) due to the high bending torque close to the established threshold value (1.3) for automotive safety.

In case 2B, there is no head contact with the metal seat handle (Fig. 5) due to the higher friction coefficient representing a dry clean bus floor ($\mu = 0.85$), and the only significant result was a predicted 39% risk of right knee fracture from the seat contact. The larger friction coefficient influenced this result, demonstrating that small changes in input parameters can result in large changes in predicted injury outcomes.

In cases 3A and 3B, the falling mechanism of the human model is similar to cases 2A and 2B (Fig. 6). However, the predicted force/torque in the femur and knees is higher now due to the high acceleration followed by a long deceleration. This represents a bus accelerating quickly from a traffic light and subsequently suddenly braking to a halt. Due to inertia, the body is pushed backward with both legs contacting the front seat border at knee level, before falling over the seat cushion. In both cases the only significant injury predictions were in the knees. Here, impacts between the legs and seat border were much closer to the knee, and torques in Simulation 3B are slightly higher because the friction coefficient is higher than in Simulation 3A (the same situation occurs between simulations

16

2A and 2B) and there is a brief period when the leg gets caught between the floor and seat border during the falling process. This is when the highest bending torques are reached: a maximum in the right knee of 137Nm, representing a 55% probability of AIS≥2 injury, the highest predicted probability for any type of injury in this paper.

In case 4A and 4B the human model was placed holding a vertical handrail in an area specially designated for standing passengers in urban buses ('Position 2'). The same acceleration input as in Simulations 3A and 3B was used. In both cases the human model fell backwards and injuries are predicted following leg contact with the floor. There is no head impact, since this area is designated for standing passengers and is clear of hazardous elements (head impact with the floor did not happen because a seated posture was maintained on the floor). Consequently, the only injuries predicted were a 35% probability of fracture in the left knee in case 4B. This shows clearly that the risk of injuries is reduced when a standing passenger occupies areas specially designated for them, because there are no hazardous bus furniture items such as rows of seats to increase injury risk. However the hard impact with the ground can lead to high risks of knee fracture and probably hip injuries, so passengers need more restraint elements like handles to reduce the risk of falling. Hip injuries were not evaluated here but should be a focus of future work. Ideally, standing passengers would not be allowed and this area would be filled with more seats.

Direct comparison of the model predictions with real world cases is not possible since the bus acceleration time history for individual accident cases is not available. Furthermore, real world leg and head injury trauma are reported only as a percentage of the total injuries. However, the model prediction of up to 55% probability of AIS≥2 knee injury and up to 35% risk of skull fracture occurring both in acceleration and deceleration bus manoeuvres

is in broad agreement with Albertsson (2005), who reported similar occupant risks arising from harsh braking and accelerating. Similarly, the bus acceleration patterns recorded in this study and used as the simulation inputs correspond well to published data study (De Graaf and Van Weperen, 1997).

6. Conclusions

This paper represents the first computational approach to non-collision bus injuries sustained by older people. Acceleration peaks and profiles were close to the threshold for balance loss and the severity of injuries predicted were in general accordance with published medical reports. Based on our analysis, the following changes are proposed for urban bus transport:

Vehicle Design and Standing Occupant Location

1. Passengers should be discouraged from standing in the aisles (to prevent leg injury risk from contact with the stiff seat frames) and immediately behind the stairwell (to prevent head contact with the stairwell wall). They should instead stand in a dedicated area opposite the stairwell and be provided with roof mounted vertical handholds. Padding in this area is important.

2. Horizontal metal seat handles should be replaced with vertical ones hung from the roof of the bus (but low enough for older shorter people to reach).

3. A lower stiffness of the rubber used for the floor should be considered.

Bus Driver Training

4. Accelerations quickly followed by harsh decelerations are frequent in urban

    buses and are likely to result in more severe injuries in the event of loss of

    balance for a standing occupant. Therefore driver training should be expanded to

    include mandatory viewing of videos based on multibody occupant simulations

    of non collision accident scenarios to demonstrate the influence of driving

    patterns on standing occupant balance loss and subsequent injury risk.

Acknowledgements

References

Albertsson, P., 2005. Occupant Casualties in Bus and Coach Traffic – Injury and Crash
    Mechanisms. Umeå University.
Albertsson, P., Björnstig, U., Björnstig, J., Bylund, P-O., Falkmer, T., Petzäll, J., 2005.
    Injury events among bus and coach occupants-Non crash injuries as important as crash
    injuries. IATSS RESEARCH, vol. 29, No. 1.
An, K., et al., 1979. Normative model of human hand for biomechanical analysis. Journal
    of Biomechanics 12, pp. 775-788.
Buchanan, T., Lloyd, D. G., Manal, K., Besier, T.F., 2004. Neuromusculoskeletal
    Modeling: Estimation of Muscle Forces and Joint Moments and Movements from
    Measurements of Neural Command. J Appl Biomech 20 (4), pp. 367-395.
Canavan, M., et al., 2005. Non-collision Bus injuries: a Particular Hazard for Older People.
    Irish Journal of Medical Science 174 (2).
De Graaf, B., Van Weperen W., 1997. The Retention of Balance: An Exploratory Study
    into the Limits of Acceleration the Human Body Can Withstand Without Losing
    Equilibrium. Human Factors and Ergonomics Society 39 (1), pp. 111-118.
Don, B. van, Ratingen, M. van Bermond, F., Masson, C., Vezin, P., Hynd, D., Owen,
    C., Martinez, L., Knack, S., Schaefer, 2003. Biofidelity impact response

requirements for an advanced mid-sized male crash test dummy, Proceedings of the 18th International Technical Conference on Enhanced Safety of Vehicles.

Eppinger, R., Sun, E., Bandak, F., Haffner, M., Khaewpong, N. Maltese, M., Kuppa, S., Nguyen, T., Takhounts, E., Tannous, R., Zhang, A., Saul, R., 1999. Development of Improved Injury Criteria for the Assessment of Advanced Automotive Restraint Systems - II. National Highway Traffic Safety Administration (NHTSA).

Fruin, J., Huang, H.F., Zegeer, C.V., Smith, N.E., 1994. Recommendations for Reducing Noncollision Bus Passenger Injuries. Transportation Research Record 1433, pp. 41-48.

Funk, J.R., Crandall, J.R., Tourret, L.J. MacMahon, C.B., Bass, C.R., Khaewpong, N., Eppinger, R.H., 2001. The Effect of Active Muscle Tension on the Axial Injury Tolerance of the Human Foot/Ankle Complex. Experimental Safety Vehicles, paper 237.

Funk, J.R., Crandall, J.R., Tourret, L.J., MacMahon, C.B., Bass, C.R., Patrie, J.T., Khaewpong, N., Eppinger, R.H., 2002. The Axial Injury Tolerance of the Human Foot/Ankle Complex and the Effect of Achilles Tension. Journal of Biomechanical Engineering 124, pp. 750-757.

Gambinon, S., Mirochnik, M., Schechter, S., 2006. Center of Mass of a Human. The Physics Factbook™, http://hypertextbook.com/facts/2006/centerofmass.shtml

Golob, T., Hensher D., 2007. The trip chaining activity of Sydney residents: A cross-section assessment by age group with a focus on seniors. Journal of Transport Geography, in press.

Halpern, P., Siebzehner, M.I., Aladgem, D., Sorkine, P., Bechar, R., 2005. Non-Collision Injuries in Public Buses: a National Survey of a Neglected Problem. Emerg. Med. J. 22, pp. 108-110.

Happee, R., Hoofman, M., Kroonenberg van den, A.J., Morsink, P., Wisman, J., 1998. A mathematical human model for frontal and rearward seated automotive impact loading. In: Proceedings of the Stapp Car Crash Conference, paper 983150.

Hirshfield, C., 1932. Disturbing Effects of Horizontal Acceleration. In: Proceedings of the Electric Railway President's Conference Committee.

Ivarsson, J., Lessley, D., Kerrigan, J., Bhalla, K., Bose, D., Crandall, J., Kent, R., 2004. Dynamic Response Corridors and Injury Thresholds of the Pedestrian Lower Extremities. In: Proceedings of the IRCOBI Conference, Graz, Austria.

Jenkins, J., 2007. Transportation for Older Adults. Transportation Planning 32 (1), pp. 1-2,4-5.

Kerrigan, J., Drinkwater, D.C., Kam, C.Y., Murphy, D.B., Ivarsson, B.J., Crandall, J.R., Patrie, J., 2004. Tolerance of the Human Leg and Thigh in Dynamic Latero-Medial Bending. International Journal of Crashworthiness 9 (6), pp. 607-623.

King, A., 2001. Fundamentals of impact biomechanics: part 2 -- Biomechanics of the abdomen, pelvis, and lower extremities. Annu Rev Biomed Eng, 3, pp. 27-55.

Kirk, A., Grant, R., Bird, R., 2001. Bus and Coach Passenger Casualties in Non-Collision Incidents. Ed. V.S.R.C.I. Ergonomics, Loughborough University.

Kroonenberg A. van den, Philippens M., Cappon H., Wismans J. 1998. Human head-neck response during low-speed rear end impacts. Stapp Car Crash Conference, SAE paper 983158.

Lieber, R., et al., 1992. Architecture of Selected Muscles of the Arm and Forearm: Anatomy and Implications for Tendon Transfer. J Hand Surg [Am] 17 (5), pp. 787-798.

Ling Suen, S., Sen L., 2004. Mobility options for seniors. Transportation in an aging society. Transportation Research Board, Washington DC.

Lord, S., Sherrington, C., Menz H., 2001. Falls in Older People. Risk Factors and Strategies for Prevention. Cambridge University Press.

Manning P., Owen C., Roberts A., Oakley C., Lowne R., Wallace A. 1998. Dynamic Response and Injury Mechanism in the Human Foot and Ankle and an Analysis of Dummy Biofidelity. Experimental Safety Vehicles, ESV 98-S9-O-11.

Mathiowetz, V., Kashman, N., Volland, G., Weber, K., Dowe, M., Rogers, S., 1985. Grip and Pinch Strength: Normative Data for Adults. Arch. Phys. Med. Rehabil. 66, pp. 69-72.

Odufuwa, B., 2006. Enhancing Mobility of the Elderly in Sub-Saharan Africa Cities Through Improved Public Transportation. IATSS Research 30 (1), pp. 60-66.

O'Neill, D., Carr, D., 2006. Transport, ageing and driving. Principles and Practice of Geriatric Medicine. Ed. J.S.P.a.A. Sinclair, London: Wiley.

Pheasant, S., Haslegrave, C.M., 2006. Bodyspace - Anthropmetry, Ergonomics and the Design of Work, Taylor and Francis.

Sigler, P.A., 1943. Relative Slipperiness of Floor and Deck Surfaces. National Bureau of Standards, Washington.

Takahashi, Y., Kikuchi, Y., Konoscu, A., Ishikawa., H, 2000. Development and validation of the finite element model for the human lower limb of pedestrians. In: Proceedings of the 44th Stapp Car Crash Conference, paper 2000-01-SC22.

TNO, 2006. MADYMO Version 6.3.2 – Human Models Manual.

Vilenius, A.T.S., et al., 1994. A method of estimating linear and angular accelerations in head impacts to pedestrians. Accident Analysis & Prevention. 26 (5), pp. 563-570.

Yamada, H., 1970. Strength of biological materials. Baltimore, MD: Williams & Wilkens.

Appendix A

Estimation of the shoe floor contact stiffness

The following assumptions were made:

- The shoe is much less stiff than the floor, and shoe stiffness therefore governs the shoe-floor contact characteristic.

- There are four contact areas (heel and toe of each foot): the static force per contact area is $= 75.7\text{kg x }9.81\text{m/s}^2/4=185.7\text{N}$.

- There is 10% compression of the shoe material which has a static thickness of 6mm, implying a compression of 0.6mm in the shoe.

- Each contact has a linear stiffness: therefore $k = 185.7\text{N}/0.0006\text{m} = 309\ 423\text{N/m}$.

Appendix B

Static deflection of the seatframe joint

The test was performed applying successive loads of 100N increments on the seatback while the seat cushion was fixed to a table by two anchorages. The joint angular deflection is $\alpha = \arcsin\left(\dfrac{d-a}{L}\right)$, where d is the distance of the joint from the ground, a the distance of the end of the lateral frame from the ground and L the length of the lateral frame. The parameters d and L were measured. The applied torque on the joint is

22

$T = F_n \cdot \dfrac{L}{2} = (W \cdot Cos\alpha) \cdot \dfrac{L}{2}$. The resulting load-angular deflection characteristic (T-α) was implemented in Madymo. A damping coefficient ($C_d = 842$Ns/m) was also included to reduce oscillations.

Force deflection characteristic of the seatback handle

The horizontal seatback handle was divided into central and edge regions, since the edges are stiffer for bending (theory of beams). Force deflection tests were performed using a universal testing machine Instron 5589 applying variable loads in these two regions. Linear results were obtained: 167kN/m for the central section, 894kN/m for the border region and these were used in the contact definitions with these seat regions.

Cushion and seat back foam deformation

The bus seats were made of wood and foam, and covered by fabric. For the tests, a 25 cm^2 section of foam was subjected to a continuous loading/unloading cycle using a universal testing machine Instron 1011. The resulting loading/unloading behaviour was used in a hysteresis stress based seat cushion contact definition.

Figure legends

Fig. 1. Passenger position and age/gender in non-collision bus injuries in Britain from 1994 to 1998, adapted from Kirk et al. (2001).

Fig. 2. Madymo model of the interior of a common urban bus, and occupant positions investigated.

Fig. 3. Representative bus acceleration pulses measured on urban buses.

Fig. 4. Human model behaviour in Simulation 1A.

Fig. 5. Human model behaviour in Simulation 2B.

Fig. 6. Human model behaviour in Simulation 3B.

Table legends

Table 1. Injury criteria, threshold values and literature references for injury assessment.

Table 2. Injury threshold values, probabilities and cumulative distributions for injury assessment.

Table 3. Matrix of computer simulations performed.

Table 4. Principal injury predictions obtained in the Madymo simulations.

Tables

Table 1. Injury criteria, threshold values and literature references for injury assessment.

Body part		Injury criteria	Output signal	Threshold values reference
Head	a	Head Injury Criterion, HIC 36, HIC 15	Parameter obtained after integrating resultant head acceleration between different time periods: 36 and 15 ms	NHTSA Injury Criteria for the 50%[th] percentile male (Eppinger et al., 1999)
Femur	b	Femur Force Injury Criterion , FFC	Compression axial force. Duration of the maximum force	NHTSA Injury Criteria for the 50%[th] percentile male (Eppinger et al., 1999)
	c	-	Femur bending torques	Dynamic bending failure experiments (latero-medial-3-point bending) on thighs (at the mid-shaft) from PMHS, estimated for the 50%[th] percentile male (Funk et al.., 2002)
Knee	d	-	Knee dynamic valgus bending torques	Dynamic symmetric valgus 4-point bending failure experiments on knees from PMHS, estimated for the 50%[th] percentile male (Ivarsson et al., 2004)
Tibia	e	-	Tibia bending torque	Dynamic bending failure experiments (latero-medial-3-point bending) on legs (at the mid-shaft) from PMHS, estimated for the 50%[th] percentile male (Funk et al.., 2002)
	f	-	Tibia axial force	Dynamic axial impact failure tests on isolated lower extremities from PMHS, estimated for the 50%[th] percentile male (Kerrigan et al., 2004)
	g	Tibia Index (TI)	Parameter that combines bending torque and compressive axial force	NHTSA Injury Criteria for the 50%[th] percentile male (Eppinger et al., 1999)

Table 2. Injury threshold values, probabilities and cumulative distributions for injury assessment.

Body part		Output signal	Threshold value s	% Probability of injury	AIS	Probability distribution
Head	a	HIC 36 ms HIC 15 ms	1 000 700	47 % 31 %	2	$p(AIS \geq 2) = N\left(\dfrac{\ln(HIC) - 6.96352}{0.84664}\right)$
Femur	b	Compression axial force	Fz = 10 kN	35%	3	$p(AIS = 3) = \dfrac{1}{1 + e^{(5.795 - 0.5196 \cdot F)}}$
	c	Bending torques	Mxx (Latero-Medial) = 317 – 502 Nm Myy (Posterior-Anterior) = 290 – 483 Nm	8 - 76% 6 – 68 %	3	$p(AIS = 3) = 1 - e^{-e^{6.24242 \cdot Ln(M) - 38.45762}}$
Knee	d	Dynamic valgus bending torques	Mzz (Latero-Medial) = 110 – 180 Nm	20 - 98%	3	$p(AIS = 3) = 1 - e^{-e^{5.77248 \cdot Ln(M) - 28.624745}}$
Tibia	e	Bending torque	Mxx (Latero-Medial) = 198 – 418 Nm	5 - 97%	2	$p(AIS \geq 2) = 1 - e^{-e^{5.69112 \cdot Ln(M) - 33.05211}}$
	f	Compression axial force*	Fz = 2.574-7.349 kN	3 – 70 %	2	$S(f \mid x_i) = \exp\left\{-\exp\left[\begin{array}{l}4.99 \cdot \ln(f) - 43.7 - 0.964 \cdot gender + \\ +0.0793 \cdot age - 0.0552 \cdot mass\end{array}\right]\right\}$
	g	Tibia Index	TI = 1.3	_____	—	_____

---

* The probability distribution for the compression axial force in the Tibia is a function of the surrogate's gender. That parameter is 0 for females and 1 for males

Table 3. Matrix of computer simulations performed.

Position	Identifier	Input pulse	Friction coefficient
Position 1	1A	MEASURE 1.1	0.85
Position 1	2A	MEASURE 2.1	0.49
Position 1	2B	MEASURE 2.1	0.85
Position 1	3A	MEASURE 2.4	0.49
Position 1	3B	MEASURE 2.4	0.85
Position 2	4A	MEASURE 2.4	0.49
Position 2	4B	MEASURE 2.4	0.85

Table 4. Principal injury predictions obtained in the Madymo simulations.

Simulation Identifier	HIC_{36}	Threshold	Injury Risk (AIS≥2)	Right leg (kN,Nm)	Left leg (kN,Nm)	Threshold (kN,Nm)	Injury Risk (AIS≥2)	Left Tibia Index	Right Tibia Index	Threshold
1A	20.78		0 %	109.02	42.00		19 %	0.29	0.28	
2A	758.18		35 %	-	-		-	0.27	1.2	
2B	2.02		0 %	126.03	82.50		39 %	0.28	0.12	
3A	38.30	1000	0 %	51.75	128.80	110-180*[*]	43 %	0.27	0.30	1.3
3B	17.43		0 %	137.03	89.35		55 %	0.18	0.26	
4A	35.41		0 %	98.35	75.00		11 %	0.19	0.35	
4B	23.29		0 %	66.70	122.98		35 %	-	-	

---

[*] Minimum and maximum threshold values in the literature
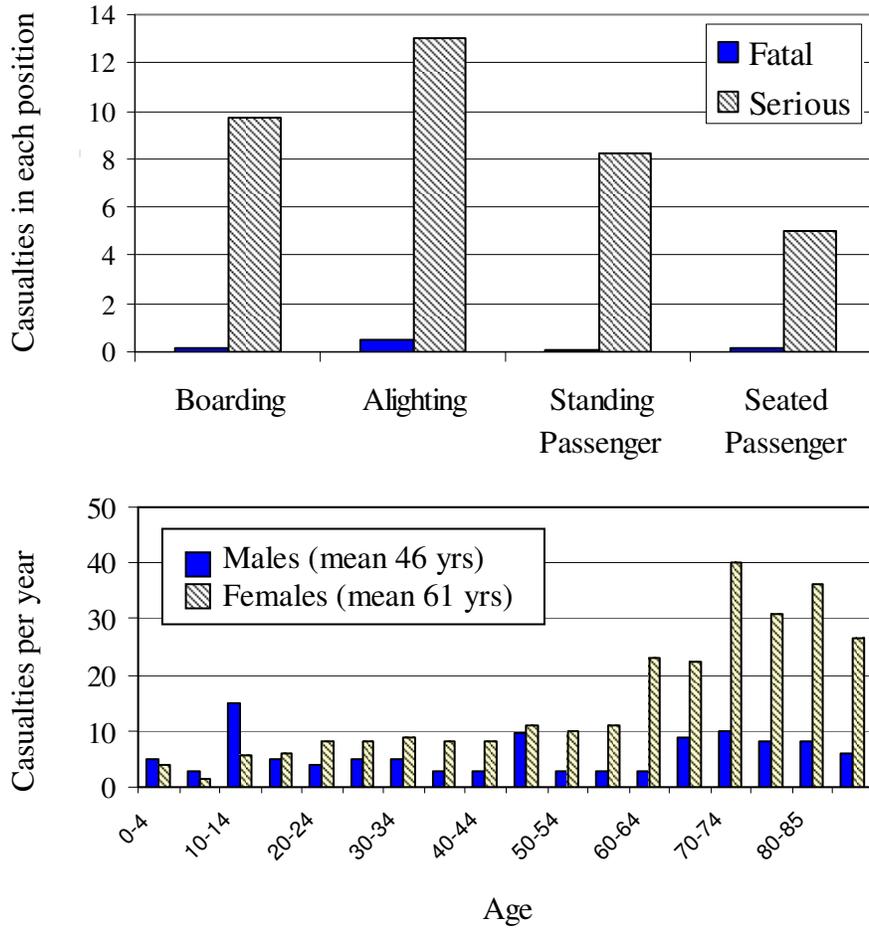
- No data available

Fig. 1. Passenger position and age/gender in non-collision bus injuries in Britain from

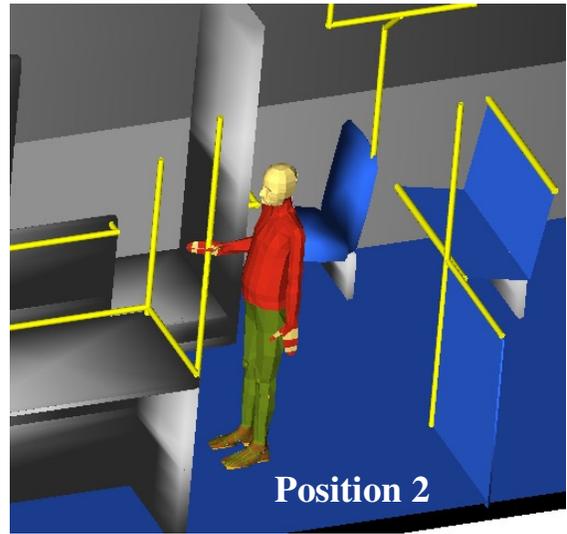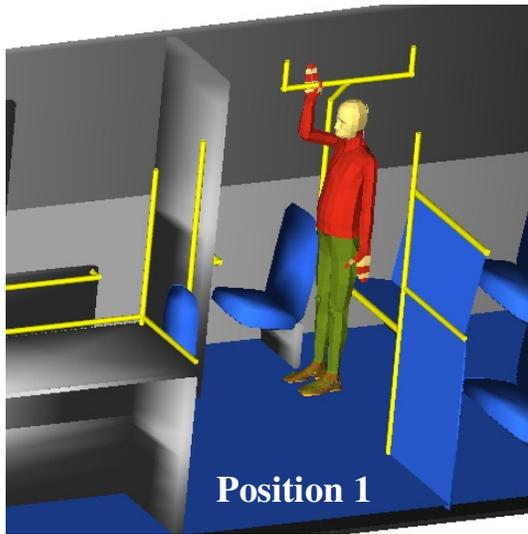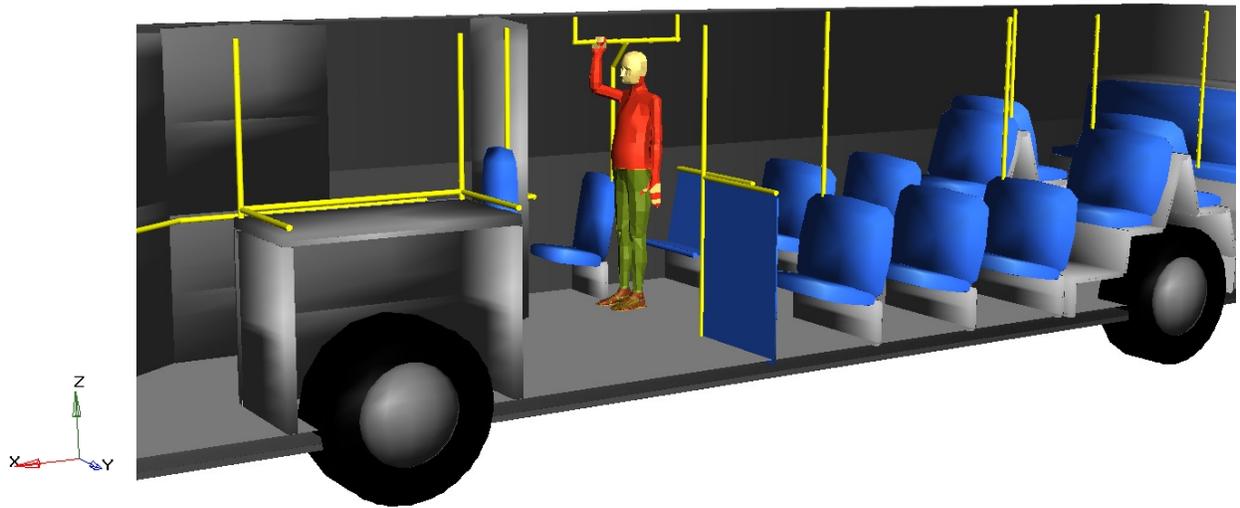1994 to 1998, adapted from Kirk et al. (2001).

Fig. 2. Madymo model of the interior of a common urban bus, and occupant positions
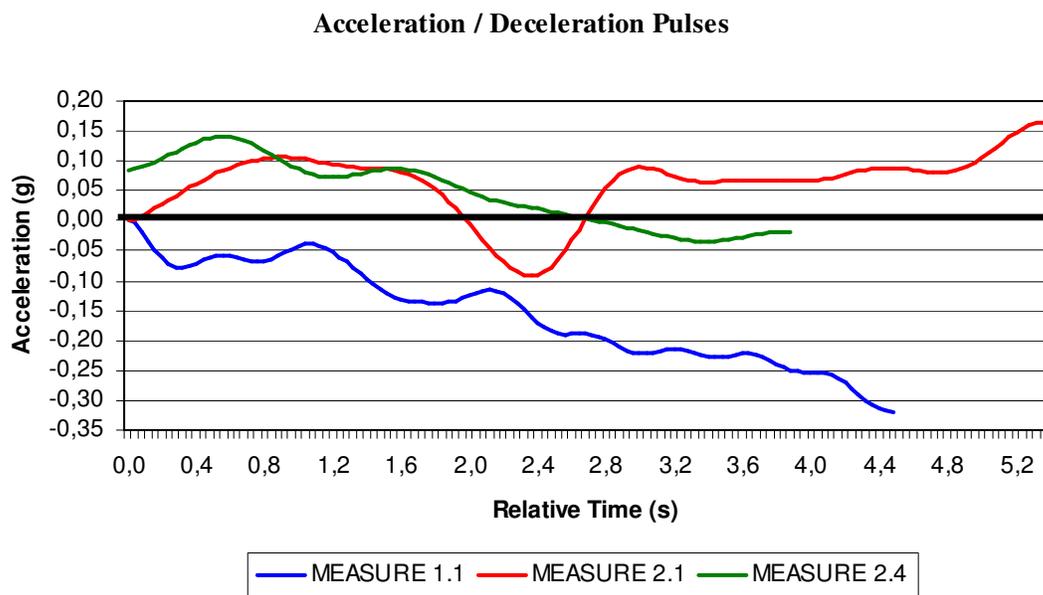
investigated.

.

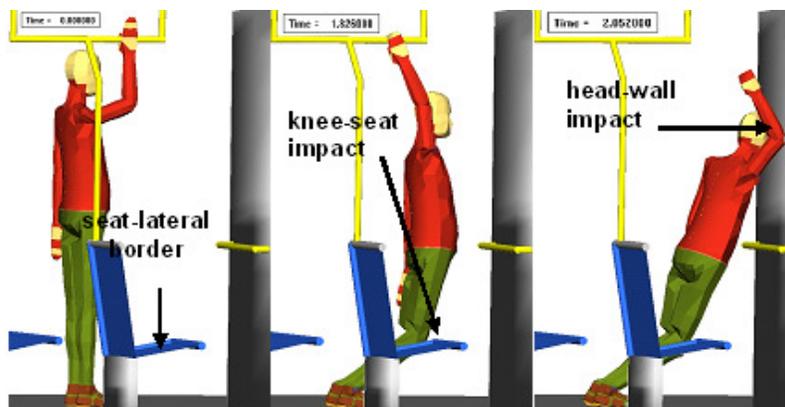Fig. 3. Representative bus acceleration pulses measured on urban buses.

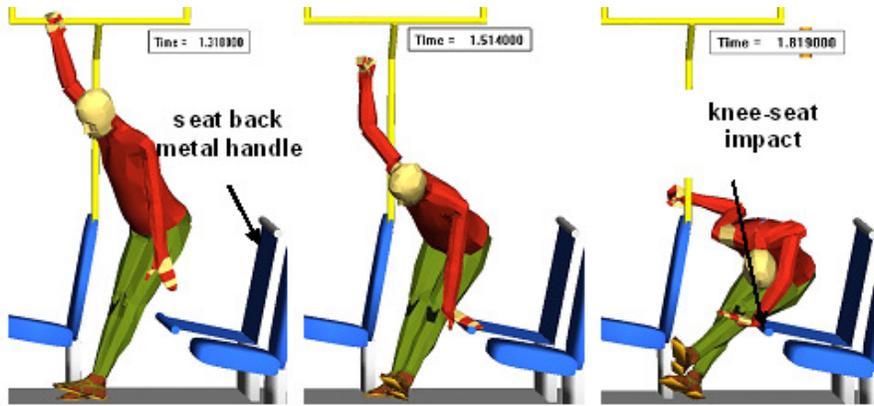Fig. 4. Human model behaviour in Simulation 1A.
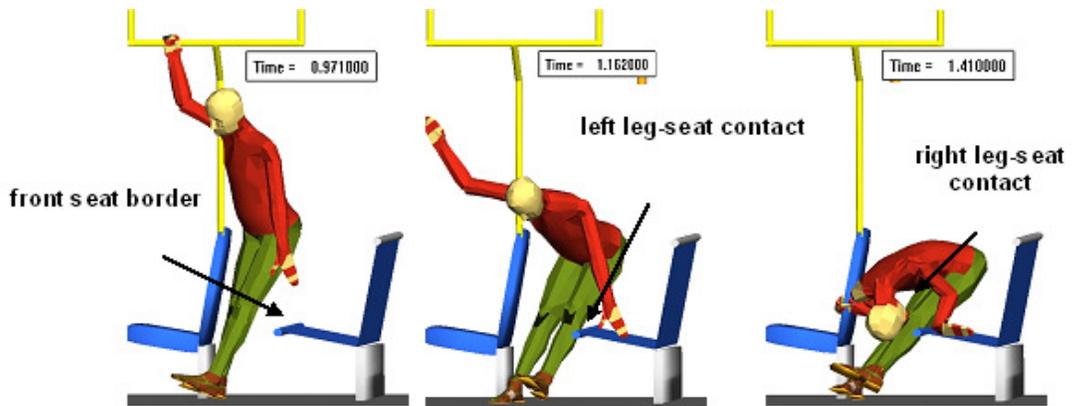
Fig. 5. Human model behaviour in Simulation 2B.

Fig. 6. Human model behaviour in Simulation 3B.